

Supporting information

An integrative temperature-controlled microfluidic system for budding yeast heat shock response analysis in single cell level

Jie Hong^{1,2}, Hao He³, Yingjia Xu¹, Shujing Wang^{1,2}, Chunxiong Luo^{1,2,3}

1The State Key Laboratory for Artificial Microstructures and Mesoscopic Physics, School of Physics, Peking University, Beijing, China

2Center for Quantitative Biology, Academy for Advanced Interdisciplinary Studies, Peking University, Beijing, China

3Wenzhou Institute, University of Chinese Academy of Sciences, Wenzhou, Zhejiang, China

*Corresponding Author:

Chunxiong Luo

The State Key Laboratory for Artificial Microstructures and Mesoscopic, Physics School of Physics, Peking University, Beijing 100871, China;

Center for Quantitative Biology, Academy for Advanced Interdisciplinary Studies, Peking University, Beijing, 100871, China; Wenzhou

Institute University of Chinese Academy of Sciences, Wenzhou, Zhejiang, 325001, China; Oujiang Laboratory, Wenzhou, Zhejiang, 325001, China; Email: pkuluocx@pku.edu.cn

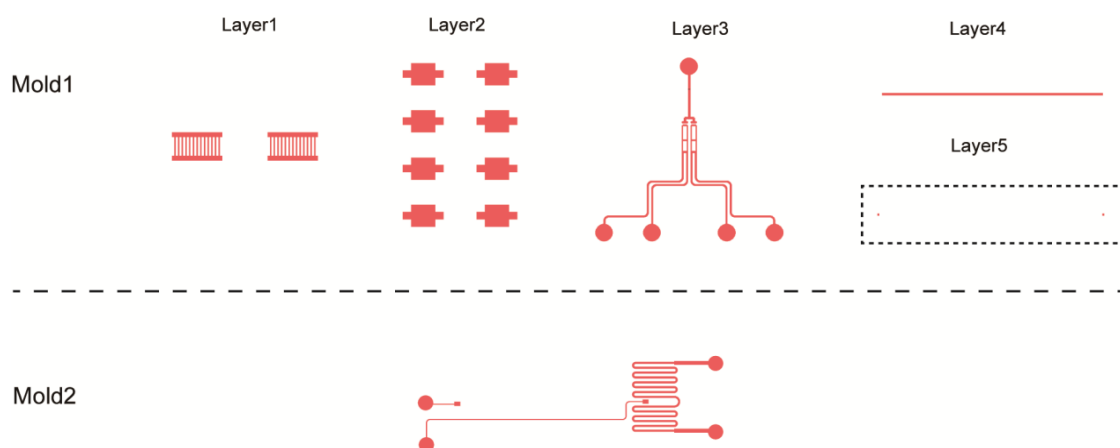


Figure S1 the detailed design of the microfluidic chip.

The above figure shows the details of the cell culture and conductive polymer layer (Mold 1) and liquid metal layer (Mold 2). Mold 1 is composed of 5 masks on the top, and Mold 2 on the bottom is composed of one mask. To clearly show the detailed pattern of each layer of the two molds, the size in the figure does not represent the true proportion of the structure. All our masks are drawn using L-edit software,

Table S1 material properties used for the multiphysics simulation

Materials	Thermal conductivity λ ($\text{Wm}^{-1}\text{K}^{-1}$)	Heat capacity C_p ($\text{J kg}^{-1} \text{K}^{-1}$)	Density ρ (kg/m^3)	Dynamic viscosity μ ($\text{Pa}\cdot\text{s}$)	Electrical conductivity σ (Sm^{-1})
Glass	1.38	703	2500	Not required	Not required
Water	0.56	4200	1000	1.01×10^{-3}	Not required
PDMS	0.15	1460	970	Not required	Not required
Air	0.026	1005	1.205	Not required	Not required
EGaln	35	367	6400	Not required	3.7×10^6
Ag@Cu-PDMS	0.8	1200	1000	Not required	Not required
Immersion oil	0.13	2197.8	800	Not required	Not required

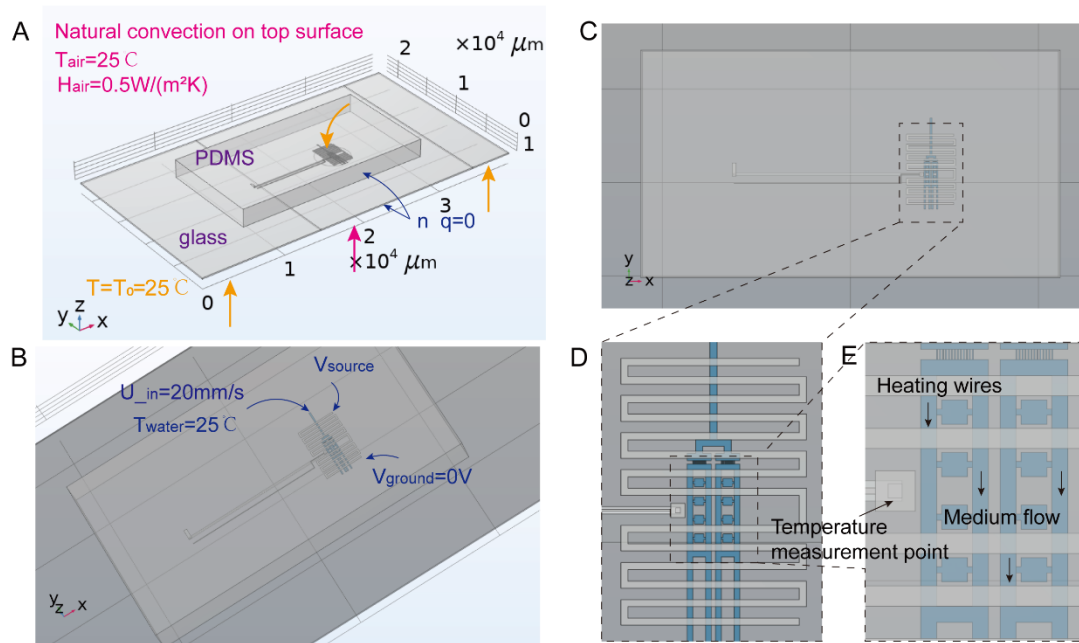


Figure S2 Detailed view of multi-physics field simulation modelling when using air objective lenses.

(A-B) The schematic of the multi-physics simulation showing initial and boundary conditions. The top surface of the model is natural convection, and the four sides are adiabatic. The bottom surface is divided into two parts. The portion of the chip that rests on metal adapters at both ends of the chip is considered to be an isothermal condition. The observation area in the center part of the chip is considered as natural convection. The initial and ambient temperatures were 25°C. The flow rate of the medium was 20 mm/s. (C-E) Zoomed in planar view of modelling detail.

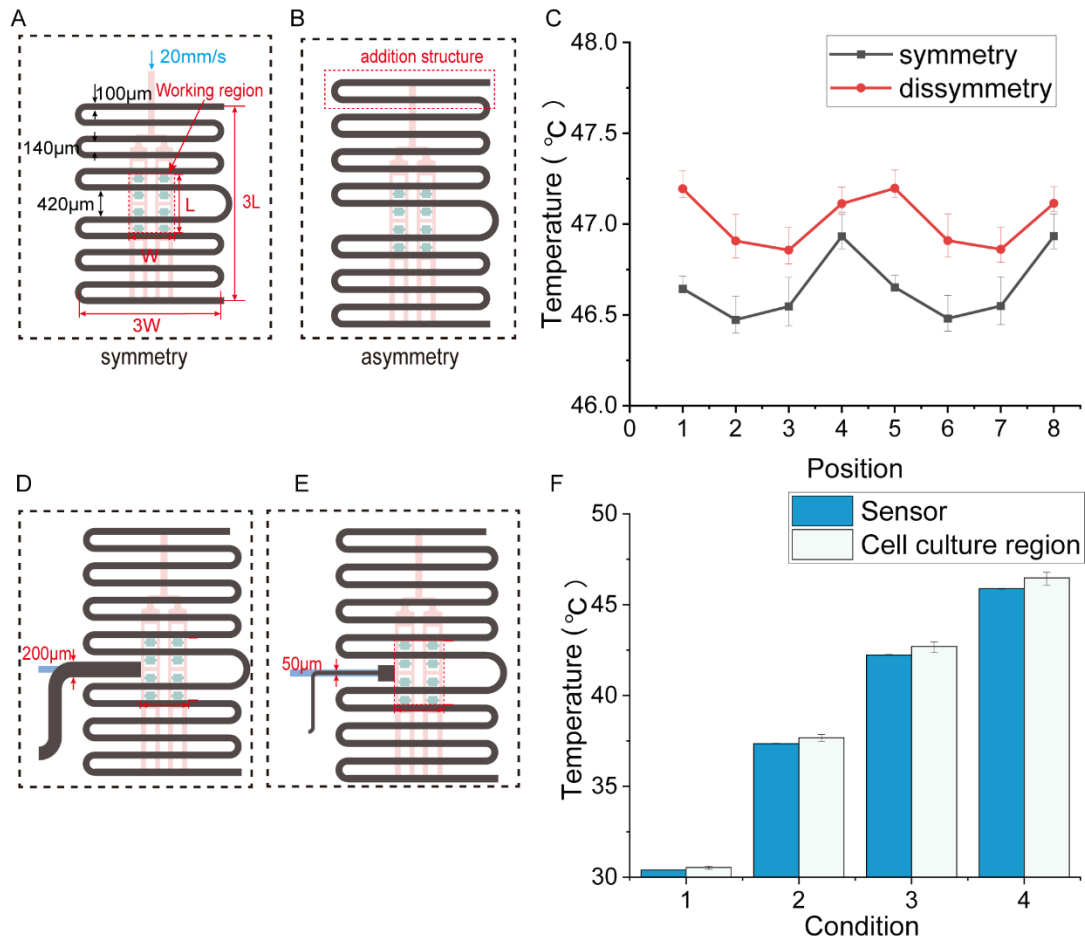


Figure S3 Effect of heating wire shape and thermocouple thickness design on the temperature field.

(A) Schematic of a symmetrical heating wire. (B) Schematic of an asymmetrical heating wire. (C) Effect of different heating wire shapes on the uniformity of temperature distribution in eight cell culture zones. The use of an asymmetric distribution at this temperature reduces the range of temperature variation by 0.3 °C in eight regions. (D) Schematic diagram of a thick thermocouple. (E) Schematic diagram of a thin thermocouple. (F) Comparison of the temperatures measured by the thick sensor and the temperatures of the eight cell culture zones at operating temperatures of 30,37,42,46°C (corresponding to four different working conditions). The upper and lower limits of the error bars represent the maximum and minimum temperatures. Maximum deviation of the measurement is 1.5°C.

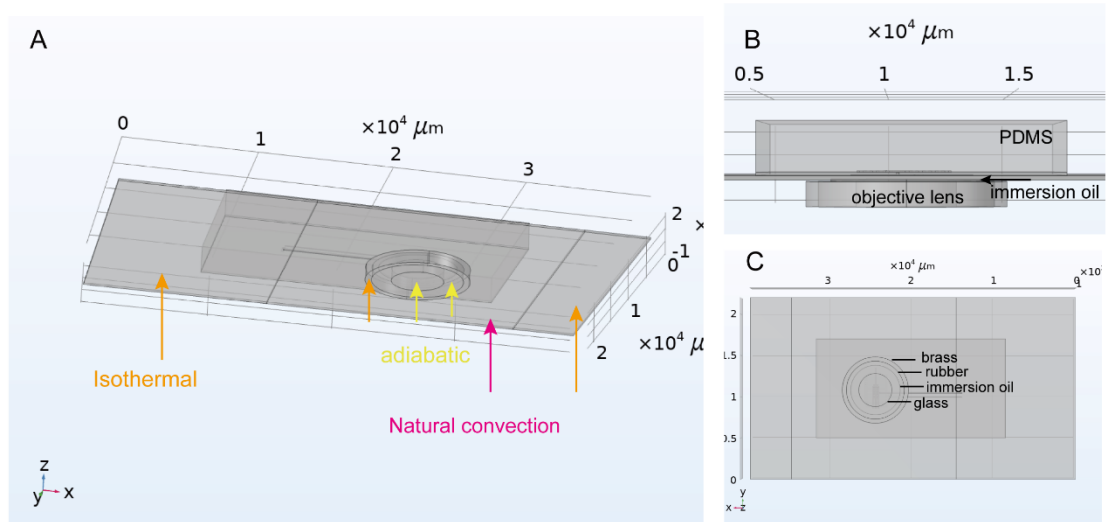


Figure S4 Detailed view of multi-physics field simulation modelling when using oil objective lenses.

(A) Schematic of the boundary conditions at the bottom of the chip. The top surface of the model is natural convection and the four sides are adiabatic. There are three types of heat transfer on the bottom surface. The ends of the chip as well as the metal part of the microscope are set to isothermal conditions. The underside of the single lens of the objective and the rubber layer are adiabatic, and the rest of the part is considered as natural convection. The initial and ambient temperatures are 25°C. (B) Front view of the multiphysics field simulation model. (C) Bottom view of the multiphysics field simulation model.

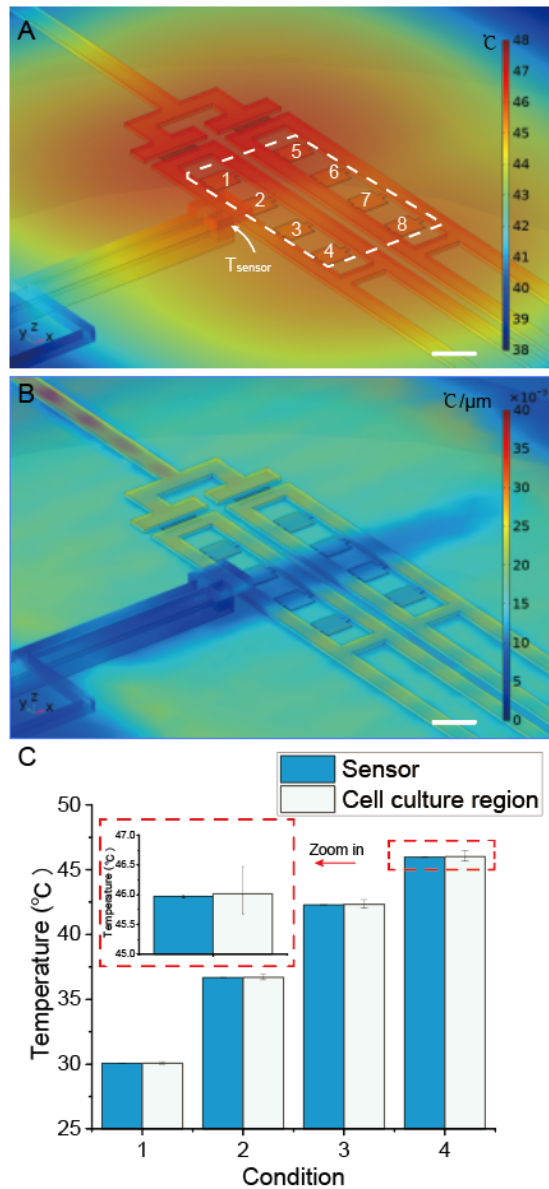


Figure S5 Multi-physics field simulation results when using oil objective lenses.

(A) Spatial temperature distribution (scale bar: 200 μm), labelling the positions corresponding to the eight cell culture regions. (B) Spatial temperature gradient distribution.

(C) Comparison between the temperatures measured by the sensor and the temperatures of the eight cell culture regions at operating temperatures of 30, 37, 42, 46 $^{\circ}\text{C}$ (corresponding to four different working conditions). The upper and lower limits of the error bars represent the maximum and minimum temperatures. At an operating temperature of 46 $^{\circ}\text{C}$, the temperature difference between the eight cell culture chambers was about 0.8 $^{\circ}\text{C}$. The temperature measured by the sensor was only 0.1 $^{\circ}\text{C}$ lower than the average temperature of the eight culture chambers.

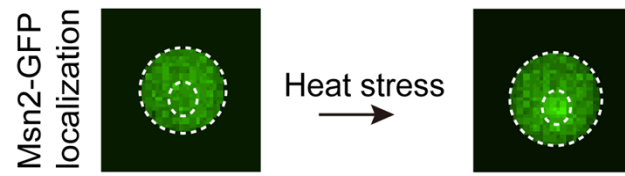


Figure S6 Schematic representation of the nuclear location of Msn2-GFP.